Research Article

Sami Bawazeer, Ibrahim Khan, Abdur Rauf*, Abdullah S. M. Aljohani, Fahad A. Alhumaydhi, Anees Ahmed Khalil, Muhammad Nasimullah Qureshi, Laiba Ahmad, and Shahid Ali Khan

Black pepper (*Piper nigrum*) fruit-based gold nanoparticles (BP-AuNPs): Synthesis, characterization, biological activities, and catalytic applications – A green approach

https://doi.org/10.1515/gps-2022-0002
received September 05, 2021; accepted November 22, 2021

Abstract: As compared to conventional techniques, currently nanotechnology has gained significant attention of scientists for the development of plant-based natural nanoparticles (NPs) due to their safety, effectiveness, and environment friendly nature. The current study was aimed for development, characterization (energy-dispersive X-ray, ultraviolet-visible spectroscopy, Fourier-transform infrared spectroscopy, and scanning electron microscopy), and evaluation of the biological efficiency of black pepper (BP; *Piper nigrum*) fruit-based gold NPs (BP-AuNPs) through different *in vitro* and *in vivo* assays. BP extract revealed maximum antibacterial and antifungal potential against *Escherichia coli* (24 mm) and *Aspergillus flavus* (47 mm), respectively. However, BP-AuNPs (200 $\mu g \cdot mL^{-1}$) inhibited the urease, xanthine oxidase, and carbonic acid-II activities with a percent inhibition of 83.11%, 91.28%, and 86.87%, respectively. Further, the anti-inflammatory effect of BP extract at the dose of 100 $mg \cdot kg^{-1}$ was 72.66%, whereas for BP-AuNPs it was noticed to be 91.93% at the dose of 10 $mg \cdot kg^{-1}$. Similarly, the extract of BP and prepared AuNPs demonstrated significant ($p < 0.01$) sedative effect at all tested doses. The BP-AuNPs catalytically reduced methyl orange dye. Results suggest that BP-AuNPs possess significant biological activities, and further studies must be conducted to identify the probable mechanism of action associated with these activities.

Keywords: gold nanoparticles, black pepper (*Piper nigrum*), stability of Au-NPs, catalytic degradation of dyes, pharmacological activities

*** Corresponding author: Abdur Rauf,** Department of Chemistry, University of Swabi, Swabi, Anbar, KPK, Pakistan, e-mail: mashaljcs@yahoo.com
Sami Bawazeer: Department of Pharmacognosy, Faculty of Pharmacy, Umm Al-Qura University, Makkah, P.O. Box 42, Saudi Arabia
Ibrahim Khan, Muhammad Nasimullah Qureshi, Shahid Ali Khan: Department of Chemistry, University of Swabi, Swabi, Anbar, KPK, Pakistan
Abdullah S. M. Aljohani: Department of Veterinary Medicine, College of Agriculture and Veterinary Medicine, Qassim University, Buraydah, Saudi Arabia
Fahad A. Alhumaydhi: Department of Medical Laboratories, College of Applied Medical Sciences, Qassim University, Buraydah, Saudi Arabia
Anees Ahmed Khalil: University Institute of Diet and Nutritional Sciences, Faculty of Allied Health Sciences, The University of Lahore, Lahore, Pakistan
Laiba Ahmad: Community Medicine Department, Khyber Medical College Peshawar, Peshawar, KPK, Pakistan

1 Introduction

Application of nanotechnology in the field of imaging, sensing, and bio-medical sciences has found to be of significant importance. In medical sciences, nanotechnology has attained attention owing to its role in human, plant, and animal health. In the last few decades, nanotechnology has attained attention of scientists due to its broad spectrum usage in various areas such as food, agriculture, biomedicine, energy, electronics, and cosmetics [1–3]. Some examples regarding the application of nanotechnology in the field of medicine are tissue engineering, cancer diagnosis via magnetic resonance imaging, detection, and destruction of tumor, controlled delivery of drugs, and electroluminescent [4–10]. Drug delivery via nanoparticles (NPs) has emerged as a novel technique having promising results. NPs are being synthesized by using different biological, chemical, and physical approaches. Among these, NPs synthesized via biological means are known to be more sustainable, effective, safe, and cost efficient as compared to physically and chemically derived

NPs [11–13]. In the last few decades, numerous metals are used for synthesis of NPs [14–16] from plant extracts, fungi, bacteria, and algae [17–22]. Metallic NPs prepared from natural plant materials have reported significant antimicrobial, antioxidant, and other biological activities, owing to their small particle size, and enhanced surface area, varied shape, and altered features [13,23,24].

NPs have been used extensively in the field of medical sciences owing to their wound healing [25], antibacterial [26], ecofriendly [27], antidiabetic [28], anticancer [29], antiviral [30], and catalytic degradation properties [31]. Scientists are focused on developing noble metal-based NPs as they have shown escalated chemical and physical properties due to their electronic configuration, enhanced surface area, and reduced size. Purposely, the most commonly used noble metals are palladium, gold, silver, and platinum [32]. Among these, gold is characterized as one of the noble metals possessing a high ionic conductivity. Behavior of synthesized gold nanoparticles (AuNPs) is adjustable depending upon their surface state, shape, and size. Industrially, AuNPs are used in the production of electrocatalyts, photocatalysts, and biomedicines [33].

Piper nigrum L. (black pepper [BP]) is a perennial shrub and flowering vine belonging to the family Piperaceae. It is cultivated for its peppercorn that is dried and extensively used for seasonings and as a spice. Owing to the regular use of BP in our daily life in different culinary recipes, it is also known as "the king of spices." Fully matured berry of BP is dark red in color and is nearly 5 mm in diameter. Vietnam is the largest BP producing and exporting country as it contributes nearly 34% of the world's BP production [34]. Distinctive pungency and unique biting taste of BP is mainly due to the abundant presence of an alkaloid known as piperine [35]. Piperine interaction with human vanilloid receptor is considered to be responsible for pungent taste associated with BP [36]. Furthermore, the biosynthetic pathway of piperine has been proposed by Schnabel et al. [37]. Black and white peppers are obtained from the same fruit nevertheless processing time and technique determines the type and color of pepper. For white pepper, the peppercorns are harvested when fully ripened, and their outer husk is removed. However, BP is obtained by drying unripen whole peppercorns with their husk intact. Both black and white peppers have wide applications such as in medicine, preservatives, and spices [38,39]. BP has various reported biological activities, for instance, carminative, antioxidative, antimicrobial, cardio-protective, antiseptic, laxative, diuretic, and analgesic [39,40]. Piperine, a main unique bioactive component present in BP is documented to be a central nervous system depressant as it has shown significant anticonvulsant properties. In ayurvedic medicine, it is found to amend the functionality of the digestive system, increase appetite, and treat nausea and dyspepsia [40]. Hence, keeping in view the medicinal importance of BP and significance of NPs in drug delivery, the current study was aimed for development, characterization, and evaluation of the biological efficiency of BP (*P. nigrum*) fruit-based gold nanoparticles (BP-AuNPs). Purposely, various *in vitro* (antibacterial, antifungal, and enzyme inhibitory properties) and *in vivo* (sedative, anti-inflammatory, and antinociceptive properties) experimentations were performed to assess the biological effectiveness of prepared BP-AuNPs.

2 Experimental

2.1 Materials and methods

Dry peppercorn seeds of BP (*P. nigrum*) were obtained from the local market. All the chemicals and reagents used in the present study were of analytical grade. Methanol, deionized water, and hydrogen tetrachloroaurate trihydrate [$HAuCl_4{\cdot}3H_2O$] were purchased from Merck.

2.2 Extraction

Known weights (1,000 g) of dry seeds of BP were ground to make its powder and then soaked in 2 L of 50% alcohol for 1 week. Afterward, Whatman no. 1 filter papers were used for the filtration of crude alcoholic extracts. Later, the crude alcoholic extract was dried using rotary evaporator for the removal of alcohol from the extract. The dried extract (1 g) was diluted using deionized water followed by filtration via Whatman no. 1 filter paper. The obtained filtrate was further used in different analytical procedures.

2.3 Optimization of AuNPs of BP

For the optimization of AuNPs of alcoholic seed extract of BP, different ratios (5:1, 10:1, 20:1, 30:1, 40:1, and 50:1) of 1 mM ($HAuCl_4$) solution and extract were used. Purposely, 1 mM warm $HAuCl_4$ (gold solution) was taken in a titration flask to which obtained extract was added and stirred for 30 min at 40°C. Later, this solution was continuously stirred for 4 h. Color change of AuNPs of BP formation is shown in Figure 1.

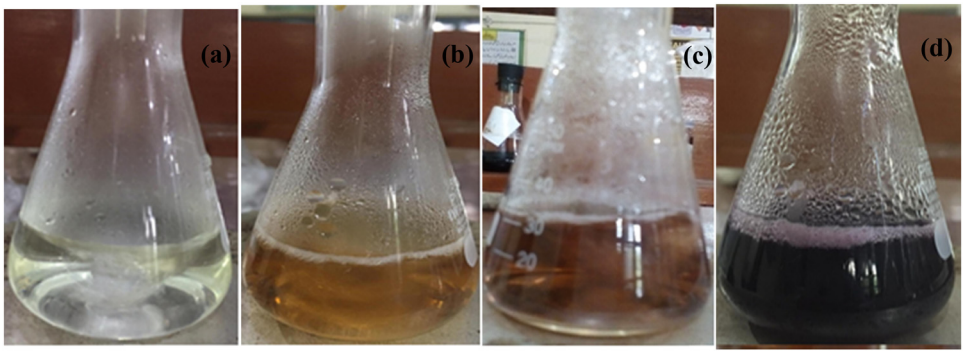

Figure 1: Color change of AuNPs of BP formation: (a) gold salt solution, (b) initial mixing of gold salt solution and extract, (c) after 30 min, and (d) after 4 h stirring.

2.4 Characterization of BP-AuNPs

Synthesized BP-AuNPs were detected via spectrophotometer (UV-Vis spectrophotometer: Shimadzu UV-1800 Japan) by placing sample in quartz at a varied wavelength. Synthesized BP-AuNPs were characterized using atomic force microscopy (AFM) and scanning electron microscope (SEM) (SM-5910-JEOL, Japan). For elemental analysis and determination of crystallinity of prepared BP-AuNPs, energy dispersive X-ray (EDX) (INCA-200, England) studies were performed. To remove unwanted components and free proteins, BP-AuNP solution was centrifuged for 15 min at 10,000 rpm. After centrifugation, the samples were vacuum dried and grounded in a mortar and pestle containing equally divided potassium bromide (KBr) to form pellets. For fourier transform infrared (FTIR) analysis, these KBr pellets were placed in a sample holder portion.

2.5 Kinetic study and stability of BP-AuNPs

In kinetic study, synthesis of BP-AuNPs with the time were studied. Purposely, samples were taken out of the reaction mixture on regular basis, and UV-data were recorded on periodic intervals. Varied conditions of parameters such as pH (2–14), salt concentration (0.1–1 M NaCl), and salt type (0.1 M NaCl, 0.1 M $CaCl_2$, 0.1 M $CuCl_2$, 0.1 M $NiCl_2$, 0.1 M Hg_2Cl_2, 0.1 M $ZnCl_2$, and 0.1 M $CoCl_2$) were studied to analyze the stability of prepared BP-AuNPs.

2.6 Catalytic activity of Au-NPs of BP

This analysis was performed to evaluate the catalytic activity of prepared BP-AuNPs in degradation of one of the most dangerous dyes present in water, that is, methyl orange (MO). MO has application in laboratories and textile industries, but due to its low biodegradability, it has become an environmental hazard [41]. MO displays maximum absorption at 464 nm in an aqueous medium. Purposely, NaBH4 solution (0.1 mM, 0.5 mL) and MO (0.02 mM, 3 mL) was placed in UV-Vis spectrophotometer cuvette. Afterward, AuNPs were added into the cuvette. Monitoring of this reaction was carried out at room temperature by using UV-Vis spectroscopy (wavelength: 200–700 nm). The decrease of absorbance at 464 nm with time was recorded by taking UV-Vis spectrum at the interval of 1 min. During the degradation process, the yellowish color of MO aqueous solution washed out and became colorless. Synthesized BP-AuNPs elevated the degradation process (MO degraded completely within 9 min).

2.7 Antibacterial activity of BP-AuNPs

Well diffusion method was followed to assess the antibacterial potential of BP extract and biosynthesized BP-AuNPs against *Escherichia coli*, *Acinetobacter*, *Streptococcus*, and *Providencia* [42]. For comparison purposes, standard drugs (norfloxacin, ciprofloxacin, levofloxacin, and amoxicillin) were used in this analysis.

2.8 Antifungal activity

Tube dilution method was adopted to evaluate the antifungal properties of BP extract and their biosynthesized AuNPs against *Alternaria solani*, *Aspergillus niger*, *A. flavus*, and *Candida albicans*. Inoculum from a fungal cultivation was added to each tube and incubated for 7 days. After incubation, tubes containing samples and standard drugs

were examined for antifungal properties. Results were expressed in percentages, and all analysis were performed in triplicates.

2.9 Urease inhibitory activity

BP-AuNPs and BP extracts were assessed for their urease inhibitory activities by following the protocols of Islam et al. [43]. For this purpose, the production of ammonia was measured via indophenol method, and thiourea was used as a standard inhibitor. Concentration of BP extract, BP-AuNPs, and standard inhibitor used in this experiment was 200 $\mu g \cdot mL^{-1}$. Data were recorded after 50 min of incubation, and percent inhibition was determined by the following formula:

$$\% \text{ Inhibition} = 100 - (\text{OD test well}/\text{OD control}) \times 100 \quad (1)$$

2.10 Xanthine oxidase activity

All the samples including BP-AuNPs and BP extracts were examined for their xanthine oxidase inhibitory activity by adopting the previously discussed experimental procedure [44]. Absorption of reaction was recorded and quantified using a spectrophotometer. Allopurinol (standard) was used in the assay mixture [44]. Concentration of BP extract, BP-AuNPs, and standard inhibitor used in this experiment was 200 $\mu g \cdot mL^{-1}$. The percent inhibition was calculated for each tested sample.

2.11 Carbonic anhydrase-II activity

BP extract and synthesized BP-AuNPs were tested for carbonic acid-II (CA-II) inhibitory potential. During this experiment, a yellow-colored compound (4-nitrophenol) was formed. This experiment was performed at room temperature and acetazolamide was taken as a standard inhibitor [45]. Concentration of BP extract, BP-AuNPs, and standard inhibitor used in this experiment was 200 $\mu g \cdot mL^{-1}$.

2.12 *In vivo* screening of BP-AuNPs

In this experimental work, Bagg Albino (BALB)/c mice procured from National Institute of Health, Islamabad, were used as a testing animal. The doses used in *in vivo* study was 10 $mL \cdot kg^{-1}$, 15–100 $mg \cdot kg^{-1}$ B.W., 2.5–10 $mg \cdot kg^{-1}$ B.W. for saline, BP extract, and BP-AuNPs, respectively.

2.12.1 Sedative activity (open-field test)

For the assessment of the sedative potential of prepared BP-AuNPs, an apparatus comprising white wood (diameter: 150 cm) with stainless steel walls was used. Base of apparatus was further divided into 19 squares with black lines. Prior to initiation of experiment, BALB/c mice were acclimatized for 1 h under dim red light. Open-field apparatus was placed in a soundproof room. Mice were divided into negative control, positive control, BP-treated, and BP-AuNPs-treated groups that were administrated with distilled water (10 $mL \cdot kg^{-1}$), diazepam (0.5 $mg \cdot kg^{-1}$), BP crude extract (15, 25, 50, and 100 $mg \cdot kg^{-1}$), and AuNPs (2.5, 5, and 10 $mg \cdot kg^{-1}$), respectively. After 30 min of administration of respective treatment, each mouse was placed in the middle of open-field apparatus for 10 min, and number of lines crossed by each mouse will be recorded [43].

2.12.2 Acetic acid-induced writhing test

This experiment was conducted to evaluate the antinociceptive potentials of BP extracts and biosynthesized BP-AuNPs. Mice were divided into nine groups, that is, Group I (negative control: distilled water; 10 $mg \cdot kg^{-1}$), Group II (positive control: diclofenac, 10 $mg \cdot kg^{-1}$), Group III (BP extract: 15 $mg \cdot kg^{-1}$), Group IV (BP extract: 25 $mg \cdot kg^{-1}$), Group V (BP extract: 50 $mg \cdot kg^{-1}$), Group VI (BP extract: 100 $mg \cdot kg^{-1}$), Group VII (BP-AuNPs: 2.5 $mg \cdot kg^{-1}$), Group VIII (BP-AuNPs: 5 $mg \cdot kg^{-1}$), and Group IX (BP-AuNPs: 10 $mg \cdot kg^{-1}$). After 30 min of administration of respective treatment, 1% of acetic acid was intraperitoneally injected to each mouse. After 5 min of injecting acetic acid, a number of abdominal constrictions (writhing) were counted for 10 min [46].

$$\% \text{ Analgesia} = 100 - \frac{\text{NWT}}{\text{NWC}} \times 100 \quad (2)$$

where NWT – number of writhing in tested animals and NWC – number of writhing in negative control animals.

2.12.3 Carrageenan-induced paw edema test

This assay was conducted to evaluate the anti-inflammatory potential of BP extracts and biosynthesized BP-AuNPs

by following the standard protocols [46]. The volume of paw edema in each mouse was recorded for five consecutive hours at an interval of 1 h after administration of inflammatory drug. For the measurement of inflammation, an instrument named plethysmometer was used. The percent inhibition in edema/inflammation was found by the following formula:

$$\text{Percent inhibition} = \frac{A - B}{A} \times 100 \quad (3)$$

where A – paw volume of negative control and B – paw volume of other tested groups.

2.12.4 Acute toxicity study

This test was performed to assess the acute toxicological profile of BP extract (100, 250, 500, and 1,000 mg·kg^{-1}) and AuNPs (10, 25, 50, and 100 mg·kg^{-1}). For 5 h, the mice were noticed for any gross changes, and then after 24 h, the mortality was recorded [47].

2.13 Statistical analysis

Outcomes of the present investigation were presented as mean ± SEM. The level of significance ($p \leq 0.05$) was evaluated using one-way analysis of variance. Afterward, for comparison purpose, Dunnett's multiple comparison test was performed.

3 Results

3.1 Optimization of AuNPs of BP

Figure 2 shows the UV-Vis spectrum of different ratios of gold solution and plant extract. The spectrum showed similar peaks at the range of 530–550 nm but having different absorbance due to different sizes of AuNPs. Based on sharpness and uniformity of peak, the 5:1 ratio showed the highest absorbance, which was the indication of greater gold black pepper nanoparticles in the solution.

3.2 Kinetic study of AuNPs of BP

Figures 3 and 4 show the kinetic study of synthesis of AuNPs of BP. It was observed that with the passage of time, the number and uniformity of NPs increase. Such observation was also plotted in the form of a graph in which absorbance was plotted against time to give almost a straight line, and from this graph, instantaneous and average rate of reaction 0.1379 m^{-1} was calculated.

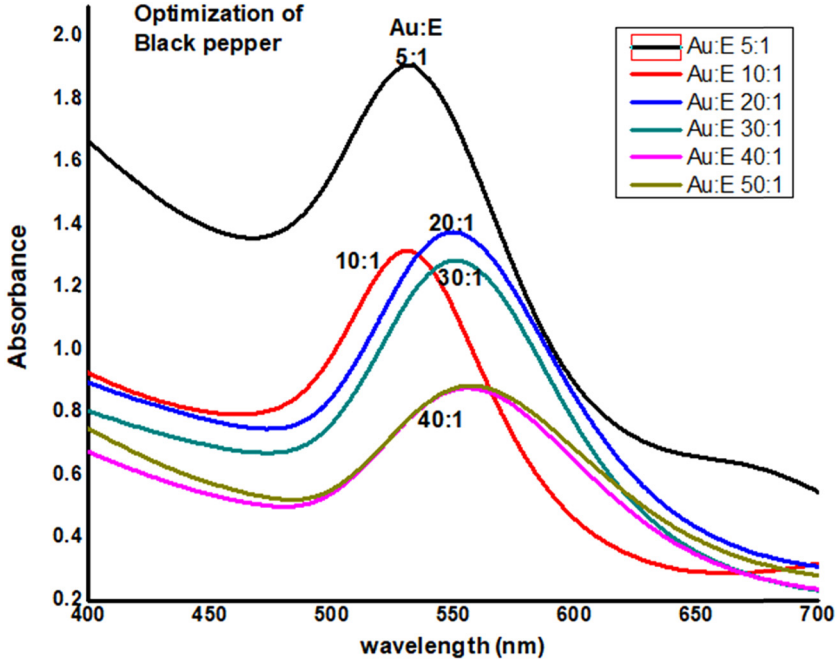

Figure 2: Optimization of AuNPs of BP.

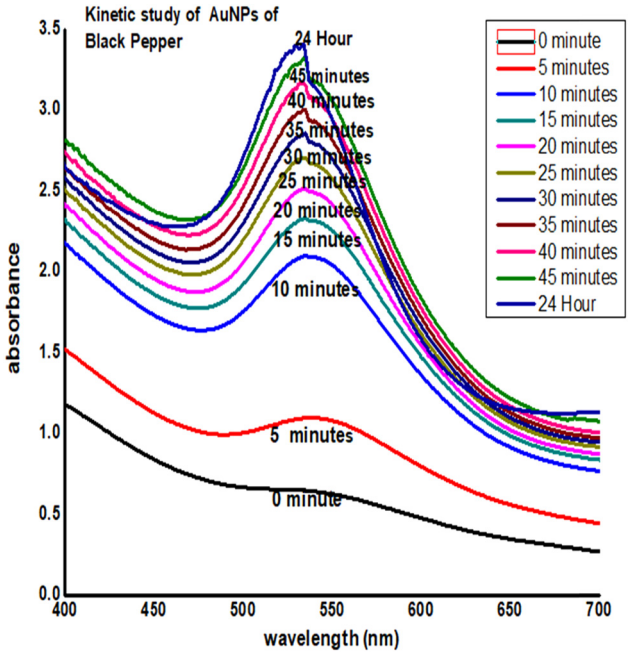

Figure 3: Kinetic study of AuNPs of BP.

3.3 Stability of synthesized BP-AuNPs

To assess the impact of varied pH on the stability of BP-AuNPs, the pH prepared solution was adjusted from 1 to 14 and then determined its affect by recording UV-Vis spectrum after 24 h. Results revealed that BP-AuNPs were found to be more stable in pH ranging from 3 to 12, whereas less stability was noticed in pH ranging from 1 to 2 and from 13 to 14. Such conclusions were drawn from the absorbance value found at different pHs as shown in Figure 5.

The effect of NaCl on BP-AuNPs was found by varying the salt concentration, that is, 0.1–1 M. UV-Vis spectra were recorded for blended salt and BP-AuNPs solution that were given hold time of 24 h. Results showed that the increase in salt concentration caused AuNPs to precipitate as a colorless solution was noticed at elevated NaCl. Addition of salt protected against the negative charges of colloidal AuNPs resulted in clumps to form large aggregates. Therefore, elevated NaCl content destabilized the synthesized AuNPs due to the removal of stabilizer as exhibited in Figures 6 and 7.

The stability of AuNPs of BP in different salt solutions (NaCl, $CaCl_2$, $CuCl_2$, $NiCl_2$, Hg_2Cl_2, $ZnCl_2$, and $CoCl_2$) was determined keeping the salt concentration constant, that is, 0.1 M. After mixing of AuNPs of BP with each salt solution in separate test tubes, UV-Vis data were recorded after 24 h. Recorded spectrums are shown in Figure 8.

3.4 Catalytic degradation of MO dye

UV-Vis spectra and kinetic study data of catalytic degradation of MO dye are shown in Figures 9 and 10. Figures show that the aqueous solution of MO gives a strong absorption peak in the visible region at 460 nm and a weak absorption peak at 282 nm. The addition of

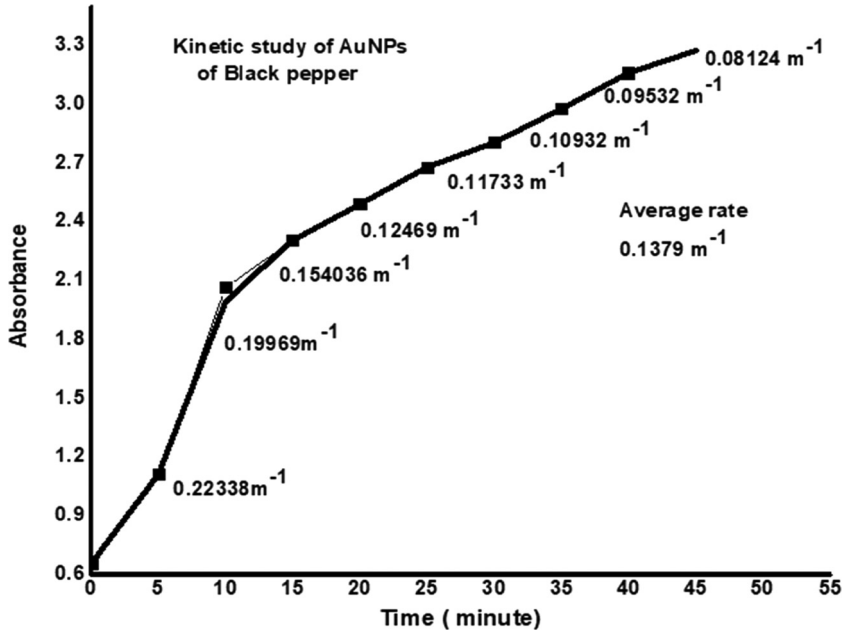

Figure 4: Rate of synthesis of AuNPs of BP.

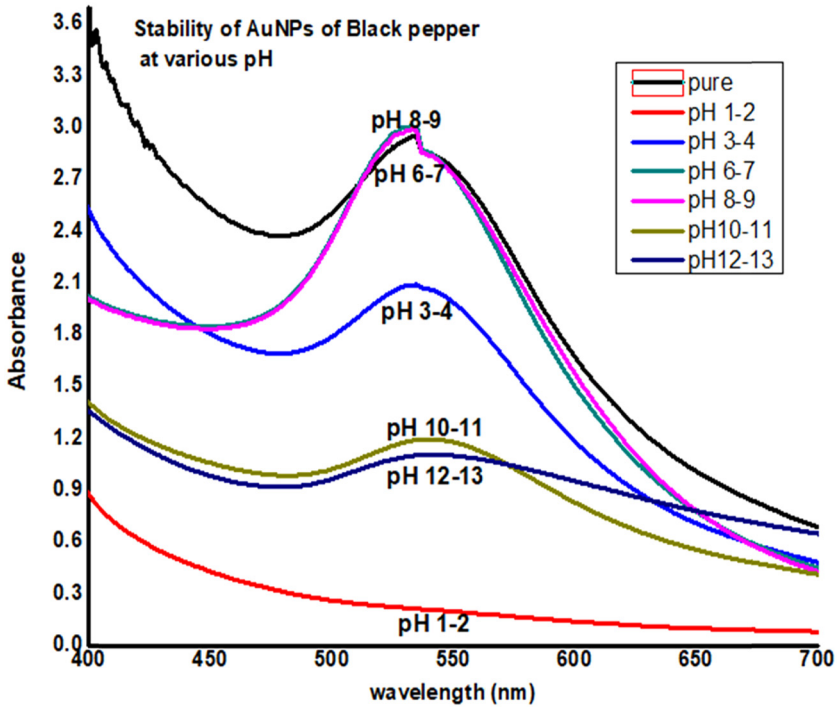

Figure 5: Stability of AuNPs of BP at various pHs.

synthesized AuNPs of BP nanoparticles enhances the reduction process. After the addition of AuNPs, the decrease in the peak intensity at 460 nm due to the beginning of MO reduction, which was completed in a short time of 9 min. Reduction in absorbance at 464 nm (wavelength) with time was documented and is shown in Figure 9. The $NaBH_4$ reduces the MO molecule at the azo site (–N═N–), which produces low molecular amino compounds. The average degradation rate was calculated, which is 0.1344 m^{-1}.

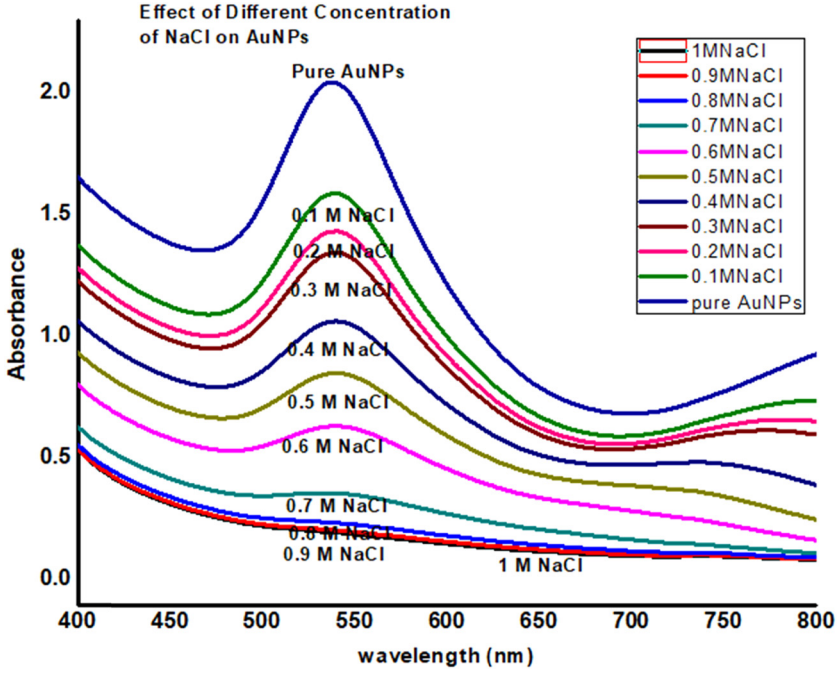

Figure 6: Stability of AuNPs of BP in NaCl (after 24 h).

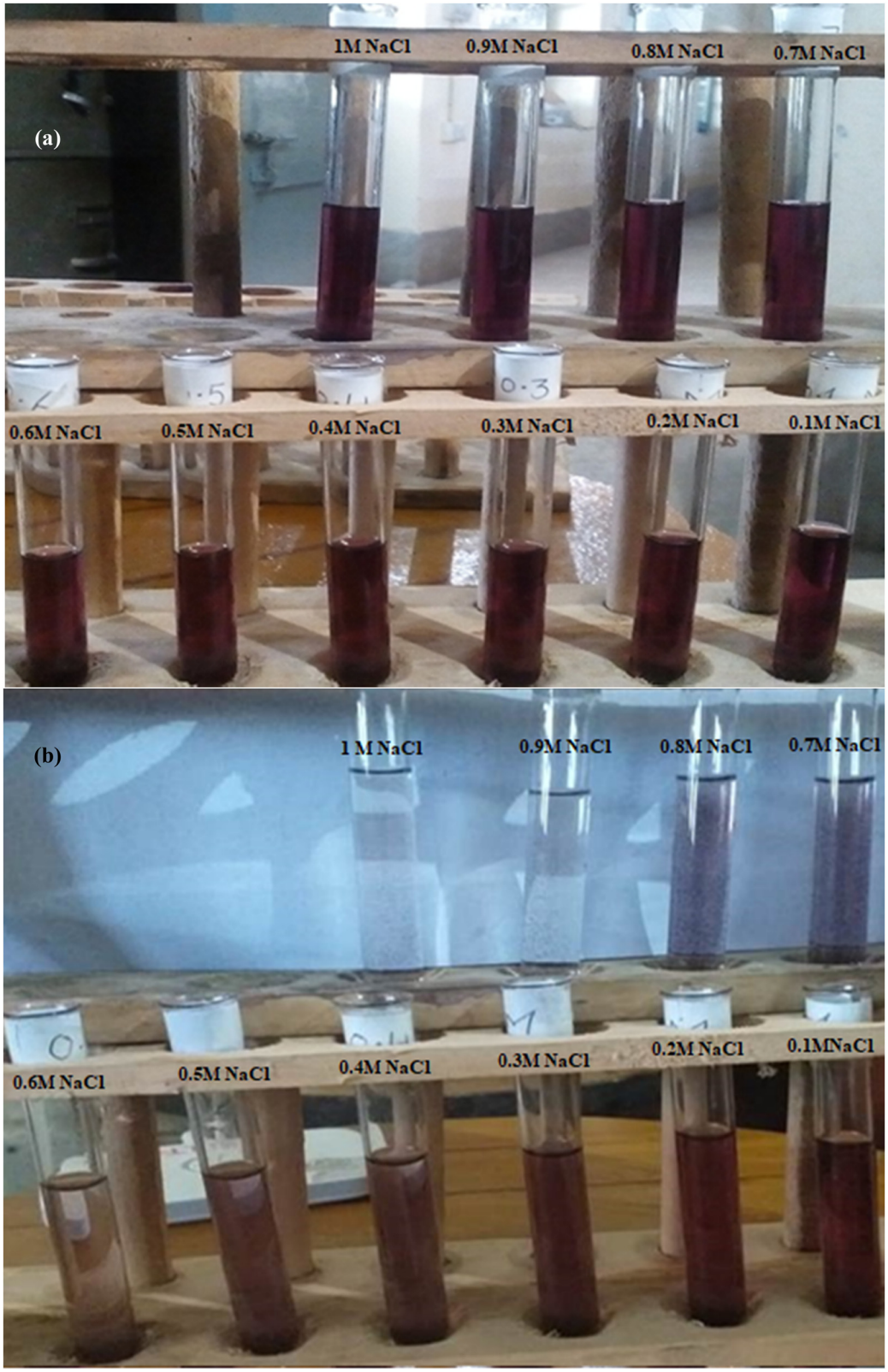

Figure 7: NaCl effect on Au NPs of black pepper after 24 h. (a) Initial mixing of salt solution with gold nanoparticles solution (b) after 24 hours of time.

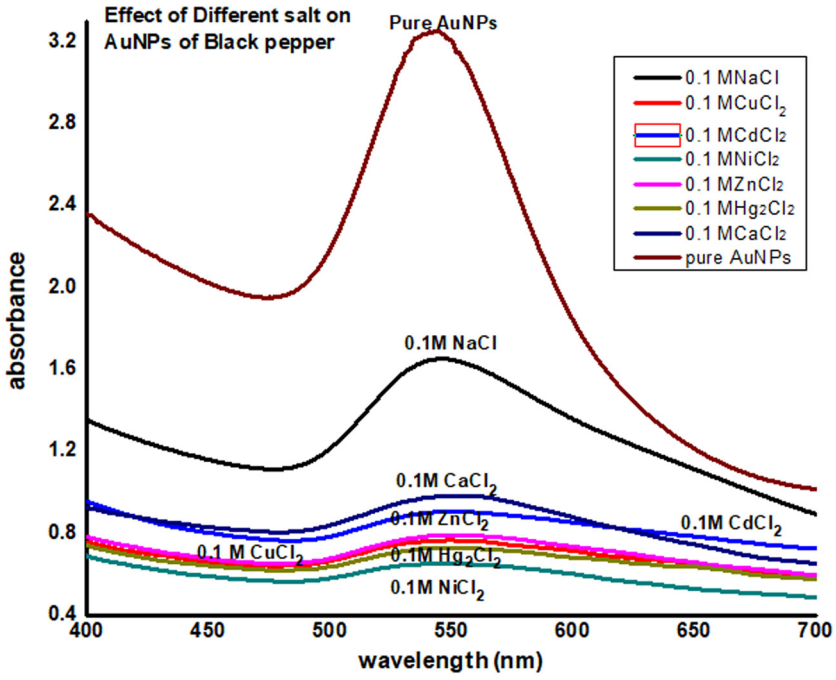

Figure 8: Stability of AuNPs of BP in different salt solutions.

3.5 Characterization of BP-AuNPs through SEM

The SEM image of AuNPs of BP showed that AuNPs were mostly spherical and oval shape having a size in the range of 40–60 nm. However, a small number of irregular NPs (nanorods, nanotriangles) were also noticed Figure 11.

3.6 Characterization of BP-AuNPs through EDX

EDX profile of AuNPs of BP show strong signals for Au atoms at 0.4 and 2.7 keV, whereas weak signals were observed at 6.2, 9.8, and 11.6 keV (Figure 12). The presence of signal for Cl in the spectrum is due to the use

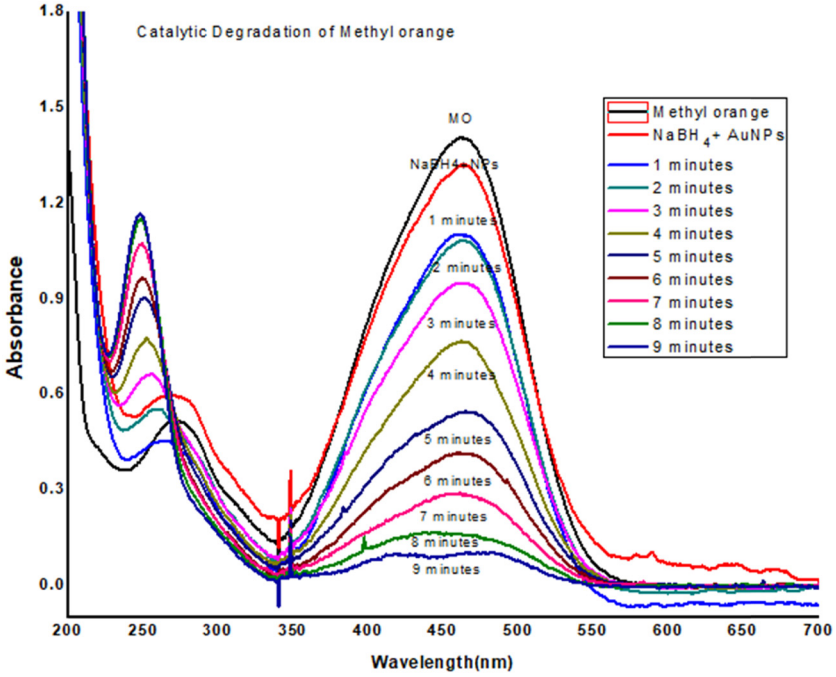

Figure 9: UV-Vis data of catalytic degradation of MO.

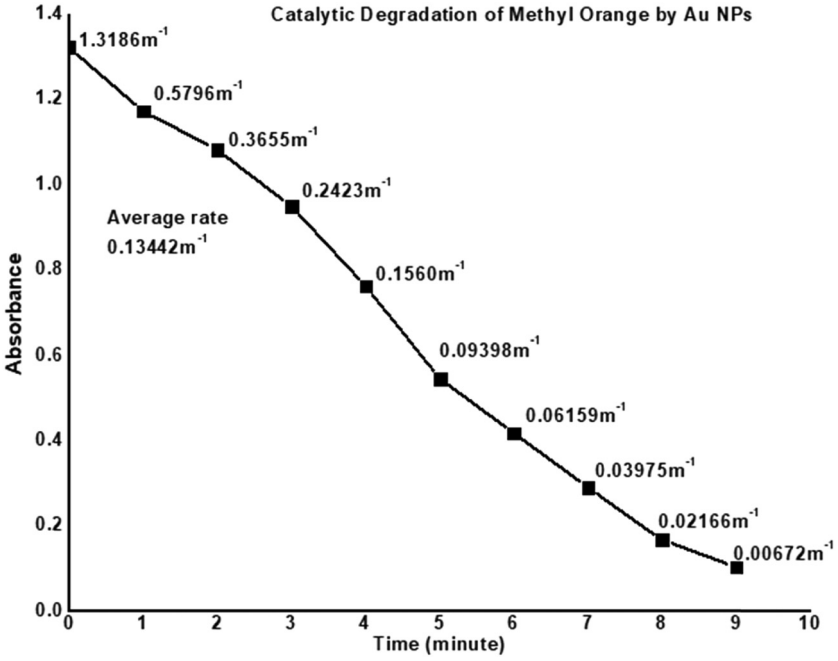

Figure 10: Kinetic study of catalytic degradation of MO.

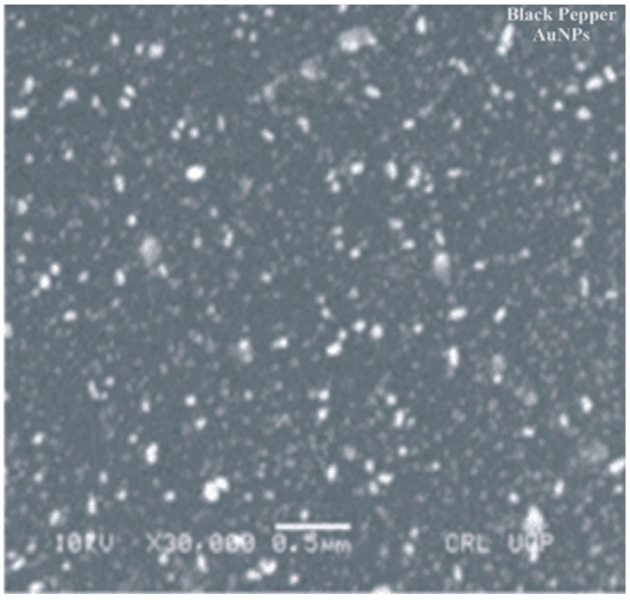

Figure 11: SEM image of AuNPs of BP.

of tetrachloroaurate salt for the synthesis of AuNPs. The appearance of Al signal corresponds to the application of Al grid in the EDX analysis, whereas the signals for C, O, and N corresponded to the presence of bio-organic molecules present in the extract that acts as a capping agent for the AuNPs. The signals for K and Mg were owing to the emission of X-ray from various biomolecules of the plant extract.

3.7 Characterization of BP-AuNPs through AFM

The AFM image of AuNPs of BP showed that the particle has an average size of 40–60 nm (Figure 13).

3.8 Characterization of BP-AuNPs through FTIR spectroscopy

Comparison of FTIR spectra of BP extract and prepared AuNPs demonstrated peak broadening in certain regions as shown in Figure 14. FTIR spectra recorded in this study showed sharp peaks with elevated amplitude at 3,417 cm^{-1} (BP-AuNPs) and 3,329 cm^{-1} (BP extract). Au^{+3} ions were reduced to Au^{0} metal due to the presence of NH or OH groups in the extract. The formation of AuNPs may be indicated due to the shift in the peak of carboxylic ketonic group from 1,728 to 1,635 cm^{-1}. Therefore, stabilization of AuNPs was related to the carboxylate group. Moreover, many differences were found in the fingerprint region of both extract and AuNPs spectra, so it is clear that BP extract is involved in reduction of gold (aurum) Au^{+3} ions from its higher oxidation state to lower oxidation state Au^{0}.

3.9 Antibacterial activities

BP extract and its AuNPs (18 $\mu L \cdot disc^{-1}$) were tested for their antibacterial activity against *E. coli*, *Acinetobacter*,

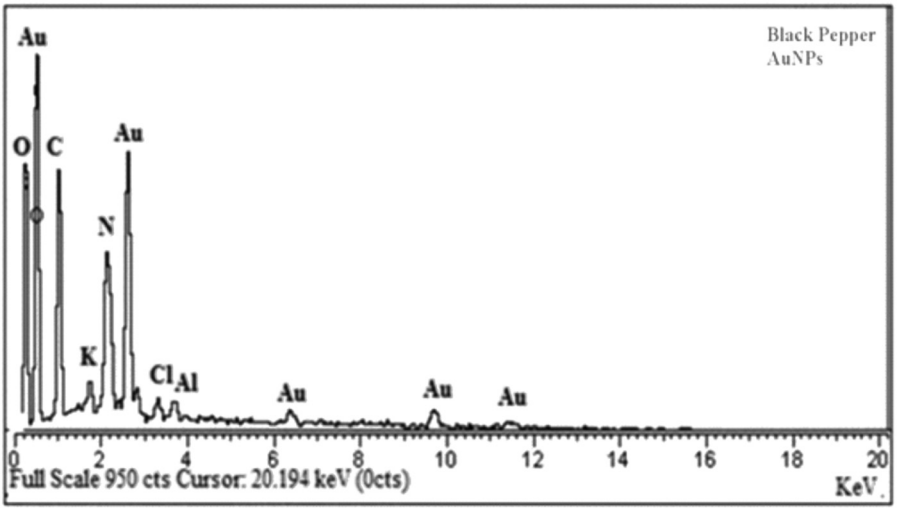

Figure 12: EDX spectrum of BP-AuNPs.

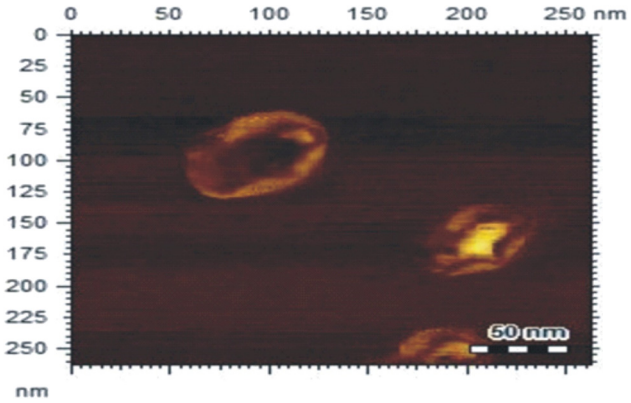

Figure 13: AFM image of BP-AuNPs.

Streptococcus, and *Providencia*, respectively. Results of antibacterial activities of BP-AuNPs and BP extract measured in millimeter are presented in Table 1.

3.10 Antifungal effect

Similarly, BP extract and its AuNPs were tested for their antifungal activity against four fungal strains. The antifungal activity of BP extract and its AuNPs are presented in Table 2; the extract observed moderate antifungal activity as compared with control. The presence of piperine an alkaloid the major constituent of piperamides present in the skin and seed of the BP is responsible for the antimicrobial activity, so it can be concluded that the extract of BP can be used as an antimicrobial agent.

3.11 Enzyme inhibition activities

Both samples (BP extract and BP-AuNPs) inhibited the urease, xanthine oxidase, and CA-II activities. Purposely, the extract demonstrated (54.38%) urease inhibitory action as compared to AuNPs (83.11%) shown in Table 3. For xanthine oxidase both the extract and AuNPs show excellent inhibitory potential of 80.76% and 91.28%, respectively. Table 4 shows the IC_{50} values of tested samples. The CA-II inhibitory potential of BP extract and BP-AuNPs were found as 60.98% and 86.87%, respectively (Table 5).

3.12 Analgesic effect of BP extract and synthesized BP-AuNPs

Analgesic properties of different experimented doses of BP extract and synthesized BP-AuNPs are exhibited in Table 6. Results demonstrated that BP-AuNPs had more analgesic activity as compared to its alcoholic extract. The analgesic and anti-inflammatory properties are due to the presence of piperine, the major component of extract.

3.13 Sedative effect

Sedative properties of different experimented doses of BP extract and synthesized BP-AuNPs are exhibited in Table 7.

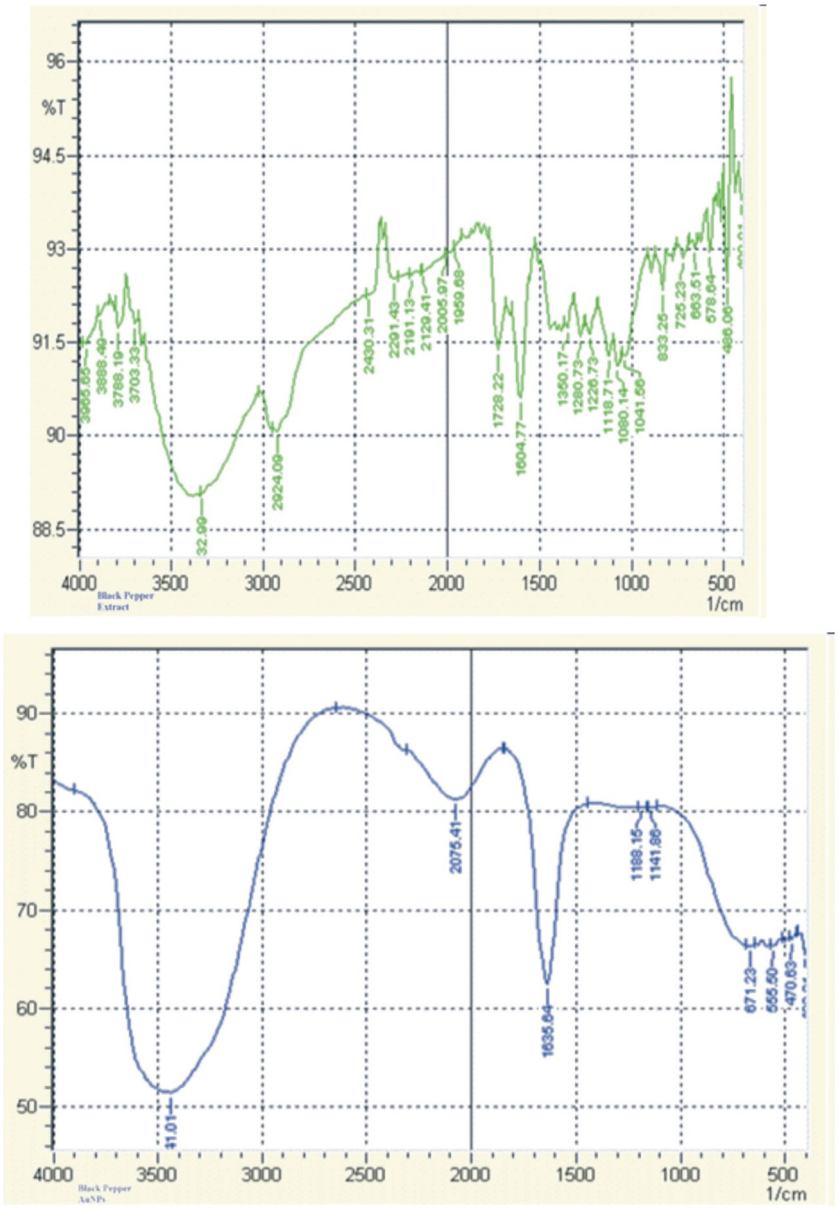

Figure 14: FTIR spectra of BP extract (green) and BP-AuNPs (blue).

Both the administrated samples revealed a significant sedative effect. The sedative effect may be due to piperine, which increased dose dependently and delayed the movement of animals at all tested doses as shown in Table 7.

Table 1: Antibacterial effect of BP extract and synthesized BP-AuNPs (zone of inhibition in millimeter)

Samples	*Acinetobacter*	*Providencia*	*Staphylococcus aureus*	*E. coli*
BP extract	10	08	21	24
AuNPs	06	07	11	13
Standard drug-1	30	25	35	22
Standard drug-2	38	27	37	19
Standard drug-3	50	35	40	19
Standard drug-4	25	16	20	30

Levofloxacin (Standard drug-1); norfloxacin (Standard drug-2); ciprofloxacin (Standard drug-3); and amoxicillin (Standard drug-4).

Table 2: Antifungal effect of BP extract and synthesized BP-AuNPs (zone of inhibition in millimeter)

Samples	*A. solani*	*A. niger*	*A. flavus*	*C. albicans*
BP extract	33	40	47	24
AuNPs	11	15	19	11
Miconazole (control)	100	100	100	100

Table 3: Effect of BP extract and synthesized BP-AuNPs against urease

Samples	Concentration ($\mu g \cdot mL^{-1}$)	% Inhibition	IC_{50} ($\mu g \cdot mL^{-1}$)
BP extract	200	54.38 ± 1.56	—
BP-AuNPs	200	83.11 ± 1.99	29.98 ± 1.21
Thiourea	200	94.95 ± 1.87	21.23 ± 0.12

BP, black pepper extract and BP-AuNPs, black pepper gold nanoparticles.

Table 4: Effect of BP extract and synthesized BP-AuNPs against xanthine oxidase

Samples	Concentration ($\mu g \cdot mL^{-1}$)	% Inhibition	IC_{50} ($\mu g \cdot mL^{-1}$)
BP extract	200	80.76 ± 0.65	96.09 ± 1.65
Au-NPs	200	91.28 ± 0.68	38.92 ± 0.94
Allopurinol	200	97.66 ± 1.54	0.59 ± 0.01

BP, black pepper extract and BP-AuNPs, black pepper gold nanoparticles.

3.14 Anti-inflammatory effect

Both tested samples, that is, BP extract and BP-AuNPs, resulted in a significant anti-inflammatory effect. The anti-inflammatory effect of BP extract at 100 $mg \cdot kg^{-1}$ was 72.66 and BP-AuNPs at 10 $mg \cdot kg^{-1}$ was found to be 91.93% while for standard 95.00%, respectively (Figure 15).

Table 6: Analgesic activity of BP extract and synthesized BP-AuNPs

Treatment	Dose (i.p.)$^{-1}$	% Inhibition of writhing
Saline	10 $mL \cdot kg^{-1}$	—
Diclofenac sodium	10 $mg \cdot kg^{-1}$	83.60 ± 0.64***
BP extract	15 $mg \cdot kg^{-1}$	38.42 ± 1.00
	25 $mg \cdot kg^{-1}$	49.60 ± 2.01
	50 $mg \cdot kg^{-1}$	61.25 ± 2.45**
	100 $mg \cdot kg^{-1}$	66.98 ± 2.99**
BP-AuNPs	2.5 $mg \cdot kg^{-1}$	64.87 ± 2.25**
	5 $mg \cdot kg^{-1}$	72.32 ± 3.20***
	10 $mg \cdot kg^{-1}$	87.23 ± 3.80***

$^{*}p < 0.05$; $^{**}p < 0.01$; $^{***}p < 0.001$.

Table 7: Sedative activity of BP extract and synthesized BP-AuNPs

Treatment	Dose (i.p)$^{-1}$	Number of lines crossed in 10 min
Saline	10 $mL \cdot kg^{-1}$	145 ± 3.44
Diazepam	0.5 $mg \cdot kg^{-1}$	8.60 ± 0.64
BP extract	15 $mg \cdot kg^{-1}$	54.5 ± 0.03***
	25 $mg \cdot kg^{-1}$	45.55 ± 3.21*
	50 $mg \cdot kg^{-1}$	35.76 ± 3.88*
	100 $mg \cdot kg^{-1}$	26.42 ± 3.66*
BP-AuNPs	2.5 $mg \cdot kg^{-1}$	89.62 ± 3.01**
	5 $mg \cdot kg^{-1}$	70.67 ± 3.14***
	10 $mg \cdot kg^{-1}$	50.98 ± 3.99***

$^{*}p < 0.05$; $^{**}p < 0.01$; $^{***}p < 0.001$.

3.15 Acute toxicity

Results of this assay showed that both the samples, that is, BP extract and BP-AuNPs, have no adverse behavioral changes and were free of mortality as given in Table 8.

4 Discussion

Herbal plants having medicinal properties are found to significantly treat different ailments. In the field of medical sciences, the concept of synthesizing, characterizing,

Table 5: Effect of BP extract and synthesized BP-AuNPs against carbonic anhydrase-II

Samples	Concentration ($\mu g \cdot mL^{-1}$)	% Inhibition	IC_{50} ($\mu g \cdot mL^{-1}$)
BP extract	200	60.98 ± 3.02	89.59 ± 2.87
Au-NPs	200	86.87 ± 2.98	43.98 ± 2.00
Acetazolamide	200	89.01 ± 1.54	18.90 ± 1.45

BP, black pepper extract and BP-AuNPs, black pepper gold nanoparticles.

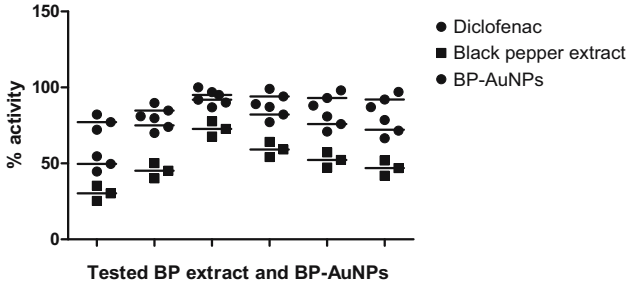

Figure 15: Anti-inflammatory effect of BP extract and BP-AuNPs on carrageenan paw edema in mice.

Table 8: Toxicological study of BP extract and AuNPs

Treatment	Dose	Number of died animals/5	% Mortality	Gross behavior changes
Normal saline	10 mL·kg^{-1}	0/5	—	—
BP extract	100	0/5	—	—
	250	0/5	—	—
	500	0/5	—	—
	1,000	0/5	—	—
	10	0/5	—	—
BP-AuNPs	25	0/5	—	—
	50	0/5	—	—
	100	0/5	—	—

and administrating natural plant-based NPs is gaining interest of scientists owing to their effectiveness and safety [48]. Plant-based NPs are preferred as their synthesis process is less elaborative [49]. Green-synthesized NPs, specifically AuNPs, have application in various fields like cosmetics, medicine, packaging, and electronics [50]. Evidently, for the synthesis of Au/Ag NPs, scientists have been using different parts of plants such as leaf, roots, stem, flower, and seeds [51]. Purposely, due to the significance of biosynthesized plant-based AuNPs, this study focused on examining the characteristics and efficiency of BP-AuNPs in various *in vitro* and *in vivo* assays.

UV-Vis spectrophotometer was used for determining the color change occurring due to the formation of AuNPs, which resulted as gold ions were reduced when reacted with BP extract. For determining the stability of biosynthesized AuNPs, UV-Vis spectrophotometer is considered to be a significant analytical tool [52]. Among all the experimented reaction mixture ratios, the maximum absorbance was noticed in case of 5:1. UV-Vis spectra showed dependency of absorption peak sharpness on extract volume ratio as highest sharpness and absorbance was noted at 5:1. Hence, bulk solution was prepared for this specific ratio owing to the efficiency in synthesis of AuNPs. The SEM and AFM analysis revealed that synthesized BP-AuNPs were predominantly in sphere and oval shape with average size ranging from 40 to 60 nm. Sadeghi et al. [53] showed that stevia leaf extract-based AuNPs had a particle size ranging from 21 to 45 nm and were spherical in shape. Similarly, Uz-Zaman et al. [54] reported that the size of synthesized *Trillium govanianum* Wall.-based NPs was between 6.5 and 65.5 nm.

UV-Vis spectra of all the examined ratios, that is, 5:1, 10:1, 20:1, 30:1, 40:1, and 50:1 for the preparation of AuNPs of alcoholic seed extract of BP showed peaks at the range of 530–550 nm. AuNPs particle size and content can be determined by using UV-Vis spectroscopy [43]. EDX analysis was performed in this investigation to assess the elemental composition of synthesized AuNPs. Outcomes of EDX analysis recorded in our study are in harmony with the previous results of Abu-Tahon et al. [55]. They concluded that at 2.2 keV strong peak was noticed as this is typical absorption of metallic AuNPs. Similarly, Alhumaydhi et al. [56] also documented strong Au peak signals at 2.3 keV. FTIR analysis conducted in this study revealed absorption bands at 3,329, 2,924, and 1,728 cm^{-1} represents $-OH/NH_2$, $-CH_2$, and C═C stretching, respectively in BP extract. However, FTIR spectra of BP-AuNPs demonstrated a shift in OH-stretching in absorption band from 3,329 to 3,417 cm^{-1} and carboxylic ketonic group from 1,728 to 1,635 cm^{-1} indicates the formation of AuNPs. Result revealed that phenols present in BP were found to be responsible for the stabilization of synthesized AuNPs [57,58].

Results of stability study conducted in this trial suggested that synthesized BP-AuNPs were most stable in pH range 3–12, whereas less stable toward highly alkaline (13–14) pH and more acidic (1–2) pH. This may be attributed to the removal of stabilizer from Au surface, therefore destabilizing the synthesized AuNPs. Further, more acidic conditions resulted in reoxidation of neutral AuNPs [59]. Stability study of BP-AuNPs toward varied concentration of NaCl demonstrated inverse relationship among salt concentration and stability of synthesized AuNPs. Maximum absorption was noticed in 0.1 M NaCl, whereas least absorption was noticed in 1 M NaCl. Alhumaydhi et al. [56] have reported similar stability results of saffron stigma-based AuNPs in varied concentration of NaCl. Similarly, Malarkodi et al. [60] also described a similar pattern of salt stress on synthesized AuNPs. Results from UV spectra showed that 1 M NaCl have the highest adverse effect on the stability of prepared NPs owing to their abrupt deteriorating effect [61]. The new peak was appeared with an increase in intensity at 250 nm, which was considered, from the

compound of the NH_2 group, which generated during the reduction of MO [62].

The development of ecofriendly, safe, and effective techniques for formulating natural therapeutic products is the foremost priority of scientists nowadays [63]. Therefore, formulation of gold and silver NPs is currently being used to synthesize plant-based NPs having boosted medicinal activities [64]. Purposely, in this study, BP extract-based AuNPs have been evaluated for their antibacterial, antifungal, and enzyme inhibitory activities. The antibacterial activity of BP extract and prepared BP-AuNPs was assessed against four strains, that is, *E. coli*, *Streptococcus*, *Providencia*, and *Acinetobacter*. Maximum antibacterial potential of BP extract was observed against *E. coli* (24 mm), whereas BP-AuNPs showed moderate antibacterial and antifungal properties against all examined bacterial and fungal strains. BP-AuNPs inhibited the urease, xanthine oxidase, and CA-II activities with a percent inhibition of 83.11%, 91.28%, and 86.87%, respectively. AuNPs loaded with plant extract acts as a sole group against microbes and, therefore, helps in elevating antimicrobial potential [65]. Maximum inhibition of bacterial strains is related to the highest content of NPs. Results of our study are in accordance with the outcomes of already published studies [66,67]. The BP extracts contain alkaloid (e.g., piperine), terpenes, flavones, and volatile oils (e.g., piperyline) that exhibit excellent antimicrobial properties and thus can be used as a food preservative [68].

Evidently, BP has been found to significantly attenuate the effect of different diseases due to phenolics present in it. In this study, acetic acid induce writhing assay was performed to evaluate the antinociceptive potential of prepared BP-AuNPs. For this purpose, BP extract (15, 25, 50, and 100 $mg{\cdot}kg^{-1}$) and biosynthesized BP-AuNPs (2.5, 5, and 10 $mg{\cdot}kg^{-1}$) at various concentrations were examined for their antinociceptive potential. Among BP extracts, the highest percent inhibition of writhing was noticed at 100 $mg{\cdot}kg^{-1}$, that is, 66.98%, whereas in case of BP-AuNPs, 87.23% inhibition was observed at 10 $mg{\cdot}kg^{-1}$. These results show that synthesized AuNPs have more potential as compared to crude BP extract. Similarly, due to the presence of BP polyphenols in its extract, the synthesized AuNPs demonstrated a significant sedative effect at all the experimented doses. Both BP extract and BP-AuNPs also showed significant anti-inflammatory potential. The anti-inflammatory effect of BP extract at 100 $mg{\cdot}kg^{-1}$ was 72.66 and BP-AuNPs at 10 $mg{\cdot}kg^{-1}$ was found to be 91.93% while for standard 95.00%, respectively. Results of acute toxicity study performed in this study showed that BP extract and BP-AuNPs were found to be free of mortality and any other unwanted behavioral changes. Anti-inflammatory and pain-killer potentials of BP and its bioactive moieties such as piperine are considered to be responsible for their analgesic effect [69]. Further, experimentations are required to authenticate the pharmacological properties of piperine. In RAW264.7 cells, piperine have found to inhibit the prostaglandin E_2 generation by suppressing the COX-2 activity [70]. Conclusion of this study reveals that BP biomolecules are potent candidates for the development of anti-inflammatory drugs. The synthesized BP-AuNPs in this study must be further evaluated to assess its mechanism of action and recommended doses in treating different diseases. BP has been administrated as anticonvulsant, antidepressant, and anxiolytic agent for treatment of neurological disorders [71]. Nanotechnology modifies the chemical, physical, and behavioral properties of metabolites by enhancing the bioactivity of plant extract, increasing the release of bioactive compound, and reducing the side effects [72]. Nanotechnology has promoted the biosynthesis of stable, effective, and nontoxic plant-based natural drugs [73].

5 Conclusion

In the field of nanotechnology, synthesis of natural NPs has gained significant importance due to their ecofriendly, safe, and efficient nature. In this study, the effectiveness of the biosynthesized BP-AuNPs was evaluated by performing different *in vitro* and *in vivo* tests. BP-AuNPs significantly reduced the growth of all the experimented bacterial and fungal strains with the maximum zone of inhibition against *E. coli* (13 mm) and *A. flavus* (19 mm). Similarly, BP-AuNPs (200 $\mu g{\cdot}mL^{-1}$) inhibited the urease, xanthine oxidase, and CA-II activities with a percent inhibition of 83.11%, 91.28%, and 86.87%, respectively. Moreover, outcomes of this study concluded that biosynthesized BP-AuNPs revealed sedative, analgesic (87.23%), and anti-inflammatory (91.33%) potentials. Further studies must be conducted to determine and understand the probable mechanism of action associated with these activities.

Acknowledgments: The study is funded by grant number 14-MED333-10 from the National Science, Technology and Innovation Plan (MAARIFAH), National Science, Technology and Innovation Plan (MAARIFAH), the King Abdul-Aziz City for Science and Technology (KACST), Kingdom of Saudi Arabia. We thank the Science and Technology Unit at Umm Al-Qura University for their continued logistic support.

Funding information: The study is funded by grant number 14-MED333-10 from National Science, Technology and Innovation Plan (MAARIFAH), the King Abdul-Aziz City for Science and Technology (KACST), Kingdom of Saudi Arabia.

Author contributions: Sami Bawazeer, Ibrahim Khan, and Abdur Rauf: conceptualization, investigation, supervision, formal analysis, methodology, validation, writing – original draft, and visualization; Abdullah S. M. Aljohani and Fahad A. Alhumaydhi: investigation, methodology, validation, and writing – review and editing; Anees Ahmed Khalil: project administration, visualization, and writing – review and editing; Muhammad Nasimullah Qureshi: formal analysis, validation, and writing – review and editing; Laiba Ahmad: formal analysis, validation, resources, and writing – review and editing; Shahid Ali Khan: data curation, formal analysis, validation, resources, writing – original draft.: data curation, formal analysis, validation, resources, and writing– review and editing.

Conflict of interest: One of the authors (Abdur Rauf) is a member of the Editorial Board of Green Processing and Synthesis.

Data availability statement: Available data are presented in the manuscript.

References

[1] Wong S, Karn B. Ensuring sustainability with green nanotechnology. Nanotechnology. 2012;23(29):290201.
[2] Roco MC, Mirkin CA, Hersam MC. Nanotechnology research directions for societal needs in 2020: summary of international study. J Nanopart Res. 2011;13(3):897–919.
[3] Kasthuri J, Kathiravan K, Rajendiran N. Phyllanthin-assisted biosynthesis of silver and gold nanoparticles: a novel biological approach. J Nanopart Res. 2009;11(5):1075–85.
[4] Panyam J, Labhasetwar V. Biodegradable nanoparticles for drug and gene delivery to cells and tissue. Adv Drug Deliv Rev. 2003;55(3):329–47.
[5] Ma J, Wong H, Kong LB, Peng KW. Biomimetic processing of nanocrystallite bioactive apatite coating on titanium. Nanotechnology. 2003;14(6):619.
[6] O'Neal DP, Hirsch LR, Halas NJ, Payne JD, West JL. Photothermal tumor ablation in mice using near infrared-absorbing nanoparticles. Cancer Lett. 2004;209(2):171–6.
[7] Aslan K, Pérez-Luna VH. Quenched emission of fluorescence by ligand functionalized gold nanoparticles. J Fluoresc. 2004;14(4):401–5.
[8] Zhong W. Nanomaterials in fluorescence-based biosensing. Anal Bioanal Chem. 2009;394(1):47–59.
[9] Narayanan KB, Sakthivel N. Heterogeneous catalytic reduction of anthropogenic pollutant, 4-nitrophenol by silver-bionanocomposite using *Cylindrocladium floridanum*. Bioresour Technol. 2011;102(22):10737–40.
[10] Rivière C, Boudghène FP, Gazeau F, Roger J, Pons JN, Laissy JP, et al. Iron oxide nanoparticle–labeled rat smooth muscle cells: cardiac MR imaging for cell graft monitoring and quantitation. Radiology. 2005;235(3):959–67.
[11] Pastoriza-Santos I, Liz-Marzán LM. Formation of PVP-protected metal nanoparticles in DMF. Langmuir. 2002;18(7):2888–94.
[12] Taleb A, Petit C, Pileni M. Synthesis of highly monodisperse silver nanoparticles from AOT reverse micelles: a way to 2D and 3D self-organization. J Mater Chem. 1997;9(4):950–9.
[13] Andreescu D, Eastman C, Balantrapu K, Goia DV. A simple route for manufacturing highly dispersed silver nanoparticles. J Mater Res. 2007;22(9):2488–96.
[14] Ahmad Z, Sharma S, Khuller GK. Inhalable alginate nanoparticles as anti-tubercular drug carriers against experimental tuberculosis. Int J Antimicrob Agents. 2005;26:298–303.
[15] Huang J, Li Q, Sun D, Lu Y, Su Y, Yang X, et al. Biosynthesis of silver and gold nanoparticles by novel sundried *Cinnamomum camphora* leaf. Nanotechnol. 2007;18:105104–15.
[16] Jhaa AK, Prasad K, Kulkarni AR. Synthesis of TiO2 nanoparticles using microorganisms. Colloids Surf B Biointerfaces. 2009;71:226–9.
[17] Dubey SP, Lahtinen M, Sillanpaa M. Green synthesis and characterizations of silver and gold nanoparticles using leaf extract of *Rosa rugosa*. Colloids Surf A Physicochem Eng Asp. 2010;364:34–41.
[18] Merin DD, Prakash S, Bhimba BV. Antibacterial screening of silver nanoparticles synthesized by marine micro algae. Asian Pac Trop Med. 2010;3:797–9.
[19] Bankar A, Joshi B, Kumar AR, Zinjardea S. Banana peel extract mediated synthesis of gold nanoparticles. Colloids Surf B Biointerfaces. 2010;80:45–50.
[20] Krishnaraj C, Jagan EG, Rajasekar S, Selvakumar P, Kalaichelvan PT, Mohan N. Synthesis of silver nanoparticles using *Acalypha indica* leaf extracts and its antibacterial activity against water borne pathogens. Colloids Surf B Biointerfaces. 2010;76:50–6.
[21] Bai HJ, Yang BS, Chai CJ, Yang GE, Jia WL, Yi ZB. Green synthesis of silver nanoparticles using Rhodobacter sphaeroides. World J Microbiol Biotechnol. 2011;27:2723–8.
[22] Santhoshkumar T, Rahuman AA, Rajakumar G, Marimuthu S, Bagavan A, Jayaseelan C, et al. Synthesis of silver nanoparticles using *Nelumbo nucifera* leaf extract and its larvicidal activity against malaria and filariasis vectors. Parasitol Res. 2011;108:693–702.
[23] Shankar SS, Rai A, Ahmad A, Sastry M. Rapid synthesis of Au, Ag, and bimetallic Au core–Ag shell nanoparticles using Neem (*Azadirachta indica*) leaf broth. J Colloid Interface Sci. 2004;275:496–502.
[24] Ali DM, Thajuddina N, Jeganathan K, Gunasekaran M. Plant extract mediated synthesis of silver and gold nano particles and its antibacterial activity against clinically isolated pathogens. Colloids Surf B Biointerfaces. 2011;85:360–5.
[25] Ahmed MK, Mansour SF, Al-Wafi R, Menazea AA. Composition and design of nanofibrous scaffolds of Mg/Se-hydroxyapatite/graphene oxide@ ε-polycaprolactone for wound healing applications. J Mater Res Technol. 2020;9(4):7472–85.

[26] Menazea AA, Awwad NS. Antibacterial activity of TiO_2 doped ZnO composite synthesized via laser ablation route for antimicrobial application. J Mater Res Technol. 2020;9(4):9434–41.
[27] Ahmed MK, El-Naggar ME, Aldalbahi A, El-Newehy MH, Menazea AA. Methylene blue degradation under visible light of metallic nanoparticles scattered into graphene oxide using laser ablation technique in aqueous solutions. J Mol Liq. 2020;315:113794.
[28] Aljabali AA, Al-Trad B, Al Gazo L, Alomari G, Al Zoubi M, Alshaer W, et al. Gold nanoparticles ameliorate diabetic cardiomyopathy in Streptozotocin-induced diabetic rats. J Mol Structure. 2021;1231:130009.
[29] Krishnan V, Bupesh G, Manikandan E, Thanigai AK, Magesh S, Kalyanaraman R, et al. Green synthesis of silver nanoparticles using Piper nigrum concoction and its anticancer activity against MCF-7 and Hep-2 cell lines. J Antimicro. 2016;2:2472-1212.
[30] Raji V, Pal K, Zaheer T, Kalarikkal N, Sabu T, de Souza FG, et al. Gold nanoparticles against respiratory diseases: oncogenic and viral pathogens review. Therapeutic Deliv. 2020;11(8):521.
[31] Menazea AA, Mostafa AM. Ag doped CuO thin film prepared via pulsed laser deposition for 4-nitrophenol degradation. J Environ Chem Eng. 2020;8(5):104104.
[32] Asiya SI, Pal K, Kralj S, El-Sayyad GS, de Souza FG, Narayanan T. Sustainable preparation of gold nanoparticles via green chemistry approach for biogenic applications. Mater Today Chem. 2020;17:100327.
[33] Menazea AA, Awwad NS, Ibrahium HA, Ahmed MK. Casted polymeric blends of carboxymethyl cellulose/polyvinyl alcohol doped with gold nanoparticles via pulsed laser ablation technique; morphological features, optical and electrical investigation. Radiat Phys Chem. 2020;177:109155.
[34] Ravindran PN, Kallupurackal JA. Black pepper. Handbook of herbs and spices. A volume in Woodhead Publishing Series in Food Science, Technology and Nutrition. Woodhead Publishing; 2012. p. 86–115.
[35] Parthasarathy VA, Chempakam B, Zachariah TJ. editors. Chemistry of spices. CAB eBooks Publisher; 2008.
[36] Schnabel A, Athmer B, Manke K, Schumacher F, Cotinguiba F, Vogt T. Identification and characterization of piperine synthase from black pepper, Piper nigrum L. Commun Biol. 2021;4(1):1–10.
[37] Schnabel A, Cotinguiba F, Athmer B, Vogt T. Piper nigrum CYP719A37 catalyzes the decisive methylenedioxy bridge formation in piperine biosynthesis. Plants. 2021;10(1):128.
[38] Thirumala-Devi K, Mayo MA, Reddy G, Emmanuel KE, Larondelle Y, Reddy DVR. Occurrence of ochratoxin A in black pepper, coriander, ginger and turmeric in India. Food Addit Contam. 2001;18(9):830–5.
[39] Wang B, Zhang Y, Huang J, Dong L, Li T, Fu X. Antiinflammatory activity and chemical composition of dichloromethane extract from *Piper nigrum* and *P. longum* on permanent focal cerebral ischemia injury in rats. Rev Bras Farmacogn. 2017;3:369–74.
[40] Mehmood MH, Gilani AH. Pharmacological basis for the medicinal use of black pepper and piperine in gastrointestinal disorders. J Med Food. 2010;3(5):1086–96.
[41] Munagapati VS, Yarramuthi V, Kim DS. Methyl orange removal from aqueous solution using goethite, chitosan beads and goethite impregnated with chitosan beads. J Mol Liq. 2017;240:329–39.
[42] Naz S, Shah S, Islam MR, Khan NU, Nazir A, Qaisar S. Synthesis and bioactivities of silver nanoparticles capped with 5-Amino-?-resorcylic acid hydrochloride dihydrate. J Nanobiotechnol. 2014;12(1):1–8.
[43] Islam NU, Jalil K, Shahid M, Rauf A, Muhammad N, Khan A, et al. Green synthesis and biological activities of gold nanoparticles functionalized with Salix alba. Arab J Chem. 2019;12(8):2914–25.
[44] Lee SK, Mbwambo ZH, Chung H, Luyengi L, Gamez EJ, Mehta RG, et al. Evaluation of the antioxidant potential of natural products. Comb Chem High Throughput Screen. 1998;1(1):35–46.
[45] Arslan O. Inhibition of bovine carbonic anhydrase by new sulfonamide compounds. Biochem (Mosc). 2001;66(9):982–3.
[46] Bawazeer S, Rauf A, Naz S, Khalil AA, Mabkhot YN, Asayari A, et al. In vivo anti-nociceptive potential and cyclooxygenases 1 and 2 selectivity of di-naphthodiospyrols from *Diospyros lotus*. Rev Bras Farmacogn. 2020;21:1–5.
[47] Rauf A, Abu-Izneid T, Rashid U, Alhumaydhi FA, Bawazeer S, Khalil AA, et al. Anti-inflammatory, antibacterial, toxicological profile, and in silico studies of dimeric naphthoquinones from diospyros lotus. Biomed Res Int. 2020;2020:7942549.
[48] Gupta AK, Gupta M. Synthesis and surface engineering of iron oxide nanoparticles for biomedical applications. Biomaterials. 2005;26(18):3995–4021.
[49] Song JY, Kim BS. Rapid biological synthesis of silver nanoparticles using plant leaf extracts. Bioprocess Biosyst Eng. 2009;32(1):79.
[50] Daniel MC, Astruc D. Gold nanoparticles: assembly, supramolecular chemistry, quantum-size-related properties, and applications toward biology, catalysis, and nanotechnology. Chem Rev. 2004;104(1):293–346.
[51] Kumar V, Yadav SK. Plant-mediated synthesis of silver and gold nanoparticles and their applications. J Chem Technol Biotechnol Int Res Process Env Clean Technol. 2009;84(2):151–7.
[52] Kasthuri J, Veerapandian S, Rajendiran N. Biological synthesis of silver and gold nanoparticles using apiin as reducing agent. Colloids Surf B. 2009;68(1):55–60.
[53] Sadeghi B, Mohammadzadeh M, Babakhani B. Green synthesis of gold nanoparticles using *Stevia rebaudiana* leaf extracts: characterization and their stability. J Photochem Photobiol B Biol. 2015;148:101–6.
[54] Uz-Zaman K, Bakht J, Malikovna BK, Elsharkawy ER, Khalil AA, Bawazeer S, et al. Trillium govanianum Wall. Ex. *Royle rhizomes* extract-medicated silver nanoparticles and their antimicrobial activity. Green Process Synth. 2020;9(1):503–14.
[55] Abu-Tahon MA, Ghareib M, Abdallah WE. Environmentally benign rapid biosynthesis of extracellular gold nanoparticles using Aspergillus flavus and their cytotoxic and catalytic activities. Process Biochem. 2020;95:1.
[56] Alhumaydhi FA, Khan I, Rauf A, Qureshi MN, Aljohani AS, Khan SA, et al. Synthesis, characterization, biological activities, and catalytic applications of alcoholic extract of saffron (*Crocus sativus*) flower stigma-based gold nanoparticles. Green Process Synth. 2021;10(1):230–45.

[57] Iravani S. Green synthesis of metal nanoparticles using plants. Green Chem. 2011;13(10):2638–50.
[58] Mittal AK, Chisti Y, Banerjee UC. Synthesis of metallic nanoparticles using plant extracts. Biotechnol Adv. 2013;31(2):346–56.
[59] Rodriguez-Sanchez L, Blanco MC, Lopez-Quintela MA. Electrochemical synthesis of silver nanoparticles. J Phys Chem B. 2000;104(41):9683–8.
[60] Malarkodi C, Rajeshkumar S, Vanaja M, Paulkumar K, Gnanajobitha G, Annadurai G. Eco-friendly synthesis and characterization of gold nanoparticles using *Klebsiella pneumoniae*. J Nanostruct Chem. 2013;3:30–7.
[61] Noruzi M, Zare D, Khoshnevisan K, Davoodi D. Rapid green synthesis of gold nanoparticles using *Rosa hybrida* petal extract at room temperature. Spectrochim Acta A. 2011;79:1461–5.
[62] Khan MM, Lee J, Cho MH. Au@ TiO_2 nanocomposites for the catalytic degradation of methyl orange and methylene blue: an electron relay effect. J Ind Eng Chem. 2014;20(4):1584–90.
[63] Chauhan RP, Gupta C, Prakash D. Methodological advancements in green nanotechnology and their applications in biological synthesis of herbal nanoparticles. Int J Bioassays (IJB). 2012;1(7):6–10.
[64] Sadowski Z. Biosynthesis and application of silver and gold nanoparticles. In: Pozo Perez D, editor. Silver nanoparticles. IntechOpen, Open Access Books Publishing; 2010. p. 257–76.
[65] Burygin GL, Khlebtsov BN, Shantrokha AN, Dykman LA, Bogatyrev VA, Khlebtsov NG. On the enhanced antibacterial activity of antibiotics mixed with gold nanoparticles. Nanoscale Res Lett. 2009;4(8):794–801.
[66] Sarvesh KS, Yamada R, Ogino C, Kondo A. Biogenic synthesis and characterization of gold nanoparticles by *Escherichia coli* K12 and its heterogeneous catalysis in degradation of 4-nitrophenol. Nano scale Res Lett. 2013;8:70–9.
[67] Logeswari P, Silambarasan S, Abraham J. Ecofriendly synthesis of silver nanoparticles from commercially available plant powders and their antibacterial properties. Sci Iran. 2013;20:1049–54.
[68] Zou L, Hu YY, Chen WX. Antibacterial mechanism and activities of black pepper chloroform extract. J Food Sci Technol. 2015;52(12):8196–203.
[69] Bang JS, Choi HM, Sur BJ, Lim SJ, Kim JY, Yang HI, et al. Anti-inflammatory and antiarthritic effects of piperine in human interleukin 1β-stimulated fibroblast-like synoviocytes and in rat arthritis models. Arthritis Res Ther. 2009;11(2):1–9.
[70] Son DJ, Akiba S, Hong JT, Yun YP, Hwang SY, Park YH, et al. Piperine inhibits the activities of platelet cytosolic phospholipase A2 and thromboxane A2 synthase without affecting cyclooxygenase-1 activity: different mechanisms of action are involved in the inhibition of platelet aggregation and macrophage inflammatory response. Nutrients. 2014;6(8):3336–52.
[71] Joshi DR, Shrestha AC, Adhikari N. A review on diversified use of the king of spices: *Piper nigrum* (black pepper). IJPSR. 2018;9(10):4089–101.
[72] Bonifacio BV, da Silva PB, dos Santos Ramos MA, Negri KM, Bauab TM, Chorilli M. Nanotechnology-based drug delivery systems and herbal medicines: a review. Int J Nanomed. 2014;9:1.
[73] Bhadoriya SS, Mangal A, Madoriya N, Dixit P. Bioavailability and bioactivity enhancement of herbal drugs by "Nanotechnology": a review. J Curr Pharm Res. 2011;8:1–7.